Microlens Laser Beam Homogenizer – From Theory to Application

Maik Zimmermann*[a], Norbert Lindlein[b], Reinhard Voelkel[c], Kenneth J.Weible[c]
[a]Bayerisches Laserzentrum GmbH, Konrad-Zuse-Str. 2-6, 91052 Erlangen, Germany
[b]Institute of Optics, Information and Photonics (Max Planck Research Group),
University of Erlangen, Staudtstr. 7/B2, 91058 Erlangen, Germany
[c]SUSS MicroOptics SA, Jaquet-Droz 7, CH-2000 Neuchâtel, Switzerland

ABSTRACT

Many applications in laser manufacturing like semiconductor lithography, micro-machining, micro-structuring or material-analysis require a homogeneous intensity distribution of the laser beam over its complete profile. Refractive and diffractive beam homogenizer solutions have been developed for this challenge, but their applicability strongly depends on the physics of the individual laser beam. This paper investigates the influence of laser beam properties like spatial coherence for microlens beam homogenizers. Diffraction at the small lens apertures and interference effects of periodic arrays are explained by using diffraction theory. Different microlens beam homogenizer configurations are presented. Design considerations that might be helpful for the layout of a specific microlens beam homogenizer system are discussed. It is shown that, among other factors, the Fresnel number is the most important quantity to characterize the influence of diffraction effects on microlens laser beam homogenizers. The influence of the spatial partial coherence will be explained for the example of a Fly's eye condenser. For cw laser sources, the influence of a rotating diffuser plate on grating interference and speckles effects is investigated. Finally, the theory will be compared to some practical examples in planar laser measurement techniques, in combustion diagnostics and micromachining with Excimer lasers.

Keywords: homogenizer, flat-top, microlens, shaping, laser, coherence, diffraction, diffuser

1. INTRODUCTION

The homogenization of laser beams is an important issue not only in many fields of laser material processing, but also in laser measuring techniques and laser analysis. Most of all, those laser applications, which image a mask pattern onto a work piece, require a homogenous distribution of radiation intensity over the whole mask area and consequently over the whole machining plane. Examples of applications are photolithographic methods for the light exposure on semiconductors [1] or the selective removal of multi layer systems. To produce multi-hole arrays, e. g. for ink-jet printer or microcavities for cupping tools [2], the diameter, the quality of the curb and the depth of the holes within the arrays must be very uniform. A beam uniformity in the range of ± 5 % (rms) is standard for laser machining applications and ± 2 % for photolithography. Similar beam quality requirements also exist for the direct radiation of a specimen with the laser, e. g. for fluorescence detection in bio-sensing. Here both beam directions are homogenized and the beam profile is mostly projected as a rectangular or squared profile on the sample.

Other applications require a homogenous thin laser line, only one beam direction is homogenized. The most important example for this application is flat-panel-display annealing. Here a thin layer of amorphous silicon is formed on a glass substrate in a vapor-deposition process. This layer must be transformed into poly-crystalline silicon. In the past, this phase transformation was performed in high-temperature ovens requiring the use of expensive, thermally resistant glass. Today, most flat-panel silicon annealing is carried out by using high-power Excimer lasers in combination with low-temperature ovens, allowing the use of low-cost glass panels. The key requirements in this application are uniform irradiation across the entire panel and a fast throughput. This is accomplished by sweeping a long, thin, highly uniform line across the panel. Further examples for thin line homogenizers are laser light sheets, e. g. for the analysis of streams and particle flow. For methods like the "Particle Image Velocimetry" (PIV) or the "Planar Laser Induced Fluorescence" (PLIV) a thin laser sheet is produced in the medium that is to be tested [3]. A quantitative precise analysis requires a homogenous distribution of intensity over the whole light-section during measuring.

*m.zimmermann@blz.org; phone +49 9131 977 90 - 28; fax +49 9131 977 90 - 11; www.blz.org

Laser Beam Shaping VIII, edited by Fred M. Dickey, David L. Shealy,
Proc. of SPIE Vol. 6663, 666302, (2007)
0277-786X/07/$18 · doi: 10.1117/12.731391

The examples above show the wide field of applications and the demand for beam homogenization. Various elements and optical systems have been developed for laser beam shaping. Hoffnagle et al. [4] described a refractive beam shaper which can be used to sort the light into a flat-top distribution using two specially designed aspherical lenses. The disadvantages of such systems are the strict dependence on the entrance profile and the proper alignment. Alignment errors and fluctuations of the laser beam have a strong influence on the achieved uniformity. Beam shaping with diffractive optical elements represents a very elegant and powerful method for the generation of arbitrary irradiation patterns [5]. These elements are usually designed for a specific wavelength and phase function. To achieve high performance, i. e. beam uniformity and efficiency, expensive multi-level elements are necessary. Another concept for flat-top generation uses multi-aperture elements, which divide the incoming beam into a number of beamlets. The beamlets are overlapped with the help of an additional lens. The advantages of these shapers are the independence from entrance intensity profile and wide spectrum of wavelengths. However, the periodic structure and the overlapping of beamlets produce interference effects especially with the usage of highly coherent light. Nevertheless a successful homogenization with these elements can be achieved with the consideration of physical optics [6] and in certain cases with the usage of additional elements like random diffusers.

2. GEOMETRICAL DESCRIPTION OF MICROLENS BEAM HOMOGENIZERS

The principle of light homogenization with arrayed elements was found more than 100 years ago. A publication of 1940 suggests the application of a multi-aperture system for the illumination in film projectors [7]. Classical homogenizers consist of lens array elements, which are produced by compression molding or manufactured through assembly of single cylindrical lenses. Classical array homogenizers have many disadvantages: manufacturing tolerances for the individual lenslets; misalignment in the array; scattering or losses at the transition and relatively high costs for mounting. Microlens arrays are a cheaper alternative which are replicated into a monolithic material of high optical quality by the use of wafer-based manufacturing processes like photolithography and reactive-ion-etching. The challenge of these processes is the optimization of the lens profile, which is essential for the quality of the homogenization [8]. However, the manufacturing costs per square millimeter are much lower compared to conventional methods.

There are two main types of microlens beam homogenizers: the non-imaging and the imaging homogenizer [9]. Both types use lens arrays to split the incident beam into beamlets. These beamlets are then passed through a spherical lens and overlap at the homogenization plane located in the back focal plane of the spherical lens. The spherical lens causes parallel bundles of rays to converge in the homogenization plane and is therefore called a Fourier lens. It carries out a two-dimensional Fourier transformation. The intensity pattern in the homogenization plane is related to the spatial frequency spectrum generated by the microlens array or arrays prior to entering the Fourier lens. The non-imaging homogenizer consists of a single lens array and a spherical lens. The imaging homogenizer with two lens arrays shown in Figure 1 usually provides much better flat-top uniformity [9].

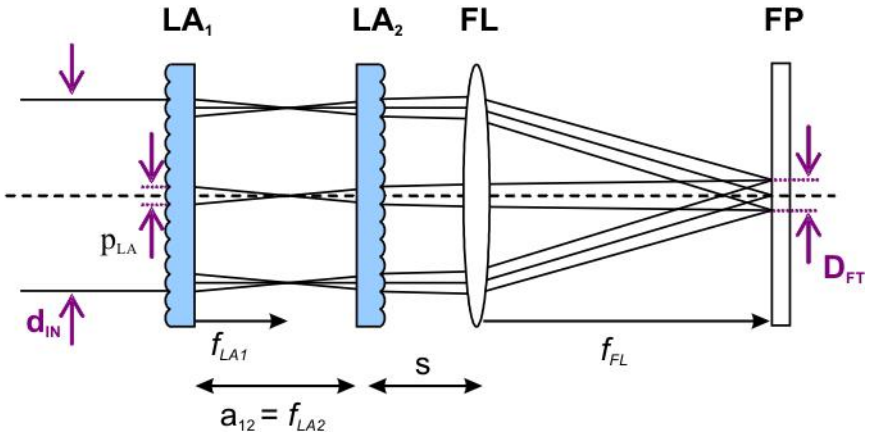

Fig. 1. Imaging Homogenizer: Two microlens arrays LA_1 and LA_2, one spherical Fourier lens FL.

The beam propagation in an imaging homogenizer is based on the Kohler illumination system which is well known from microscopy. In a fly's eye condenser, the lens arrays form many parallel Kohler illumination systems side-by-side. Multiple light sources are generated by dividing the entrance beam into multiple beamlets. The second microlens array LA_2, in combination with the spherical Fourier lens FL, acts as an array of objective lenses that superimposes the images

of each of the beamlets in the first array onto the homogenization plane FP. Square-type lens apertures of the first microlens array LA_1 generate a square flat-top intensity distribution in the Fourier plane. Circular or hexagonal microlenses will generate a circular or hexagonal flat-top, respectively. Usually square-lens or crossed cylindrical-lens arrays are used to ensure a high filling factor that is typical better than 98 %.

The lens array is characterized by the pitch p_{LA}, i. e. the vertex clearance between two neighboring lenses of the array. To show the correlation between the element-properties within the homogenizer we used paraxial matrix method for a first approximation of the geometrical optic. For the description given here, we assume a point light source at an infinite distance in front of the first lens array. The size of the flat-top D_{FT} depends on the focal lengths of the lenses within the array LA_1, LA_2 and the Fourier lens and is given by

$$D_{FT} = p_{LA} \frac{f_{FL} \cdot (f_{LA1} + f_{LA2} - a_{12})}{f_{LA1} \cdot f_{LA2}}. \tag{1}$$

To fulfil the imaging conditions as mentioned above, the separation a_{12} between LA_1 and LA_2 has to be equal to the focal length of the second lenses f_{LA2}. Through this and together with the optical power of the Fourier lens, the apertures are imaged to the plane FP. With the determination that $a_{12} = f_{LA2}$, equation (1) is simplified to

$$D_{FT} = p_{LA} \frac{f_{FL}}{f_{LA2}}. \tag{2}$$

For imaging homogenizers the divergence θ (half angle) after the homogenized plane is given by

$$\tan\theta = \frac{1}{2} \cdot \left(\frac{d_{IN} - 2 \cdot p_{LA} + D_{FT}}{f_{FL}} + \frac{f_{LA2} \cdot p_{LA}}{f_{LA1} \cdot f_{FL}} \right), \text{ with } a_{12} = f_{LA2} \text{ and } s = 0, \tag{3}$$

where d_{IN} is the diameter of the incident beam and s the distance between the second lens array and the Fourier lens. In this equation we assume that the separation s between the second lens array and the Fourier lens is zero. Normally the divergence increases by increasing this separation. Usually, imaging homogenizers consist of two similar lens arrays with identical lens pitch p_{LA} and focal length ($f_{LA1} = f_{LA2} = f_{LA}$). This configuration is the classical fly's eye condenser. For collimated laser beams, the beam is then focused into the plane of the second lens array. Thus, care must be taken not to damage the second microlens array by focusing high-power laser beams into the lens material. In this case, the focal length of the second array and according to imaging conditions the separation of LA_1 and LA_2 has to be increased. For extended laser sources like a multimode laser or a collimated fiber-coupled laser, an image of the light source is found at the plane of the second microlens array. For imaging homogenizers the diameter of the individual beamlets at the second microlens array LA_2 must be smaller than the lens pitch to avoid overfilling of the lens aperture and the loss of light. An overfilling of the second lens array results in unwanted multiple-images in the plane FP. If an extended light source with the diameter D_{source} is collimated with a positive spherical lens with a focal length $f_{CL,}$ the image size D_{image} at the second lens array is

$$D_{image} = D_{Source} \frac{f_{LA1}}{f_{CL}} \leq p_{LA}, \text{ if } a_{12} = f_{LA1} = f_{LA2}. \tag{4}$$

To avoid overfilling of lens apertures the pitch p_{LA} has to be larger than $D_{image.}$ For laser beams with a significant beam divergence the diameter of the beamlets at the second microlens array scales with the beam divergence. The allowed maximum beam divergence σ for a given microlens homogenizer is $\tan\sigma \leq \frac{p_{LA}}{2 \cdot f_{LA1}}$ for $a_{12} = f_{LA1}$.

The number of lenses N across the laser beam diameter d_{IN} is $N = d_{IN} / p_{LA}$. A simple demonstration of the intensity distribution after the homogenizer with a Gaussian entrance profile illustrates the dependence upon the number of lenses in Figure 2. For standard laser beams, an overlay of some 8 - 10 microlenses is usually sufficient to achieve a good flat top uniformity. Larger numbers of microlenses do not have negative effects. For large Excimer laser beams, homogenizers with many thousands of microlenses provide excellent flat-top profiles.

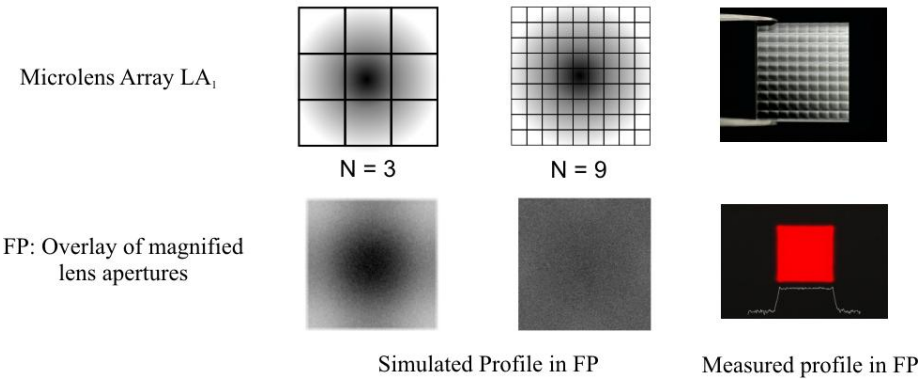

Fig. 2. Illustration of the intensity redistribution in Fourier-plane in dependence on the number of lenses.

As shown above an increasing of the number of lenslets across the pupil diameter will improve the quality of the homogeneous intensity distribution in the case of geometrical optics. Normally, the total size of the elements is limited by cost and manufacturing issues. The consequence is a miniaturization of the lenses within the array, while retaining the diameter of the incident beam. The result seen from physical optics is an increase of diffraction effects because of the smaller apertures of the lenses. For a simplified quantification of the diffraction influence, the calculation of the Fresnel number can be very helpful.

3. DIFFRACTION AND GRATING EFFECTS

A regular microlens array is a periodic structure with a period p_{LA} showing effects like grating inference and Talbot self-imaging [6, 10]. Light interacting with a periodic structure will always keep traces of this periodicity in its further propagation. This is well explained by Fourier optics: The Fourier transformation of a comb function is again a comb function. This remaining periodicity usually generates an unwanted modulation in the homogenization plane and limits the degree of uniformity that can be achieved in the flat-top. The modulation is fundamental for all refractive and diffractive laser beam homogenizers. The homogenizing process requests that the incident beam is divided into individual beamlets and that these beamlets are reorganized and overlap in the homogenization plane. Thus, the splitting of the beam itself introduces the modulation of the flat-top intensity. Obviously, the influence of these effects depends strongly on the coherence of the light source.

Using an imaging microlens beam homogenizer as shown in Figure 1 and a coherent and well collimated laser beam, the flat-top intensity profile is subdivided into sharp peaks. Due to the finite extension of the microlens array the peaks will of course not be exact delta functions, but the comb function will be convoluted with the Fourier transform of the aperture function of the illuminated part of the microlens array. The single peaks will be Airy discs if the illuminated part is circular. In the case of a Fly's eye condenser, a Fourier lens will transform the far field behind the microlens arrays into the focal plane of this lens. So, it is quite clear that in the case of coherent illumination there will be sharp peaks in the Fourier plane of the Fly's eye condenser. These peaks can only be avoided if the illumination is partly coherent or if the periodicity is avoided. Wippermann et al. [11] described a solution for avoiding the periodic structure with the help of a so called chirped microlens array. Another way to temporally smooth the spiked profile is to use rotating random diffusers.

3.1 Fresnel Number

A simple illustration and quantification of the effect of diffraction can be given by calculating the Fresnel number *FN* of the Fly´s eye condenser (Fig. 3). The Fresnel number of a lens is an important quantity to characterize the influence of diffraction effects onto the lens. The Fresnel number describes the number of Fresnel zones of a spherical wave which is formed by a lens with a diameter D_{lens} (we assume that $p_{LA} = D_{lens}$ for a filling factor of 100%) for an incident plane wave with wavelength λ.

This can be seen easily by calculating the optical path length difference (*ΔOPD*) between a ray at the rim of the lens and at the centre of the lens:

$$\Delta OPD = \sqrt{\left(D_{lens}/2\right)^2 + {f_{LA}}^2} - f_{LA} \approx \frac{\left(D_{lens}/2\right)^2}{2 f_{LA}} = FN\frac{\lambda}{2} \quad , \tag{5}$$

where f_{LA} is the focal length of a microlens within an array. Here, the square root was expressed by the first two terms of its Taylor series for the case $D_{lens}/2 << f_{LA}$. When this condition is fulfilled we can define the Fresnel number of a lens with a focal length f_{LA} and a lateral diameter D_{lens} of the lens, the Fresnel number *FN* to be:

$$FN = \frac{\left(D_{lens}/2\right)^2}{\lambda \cdot f_{LA}}. \tag{6}$$

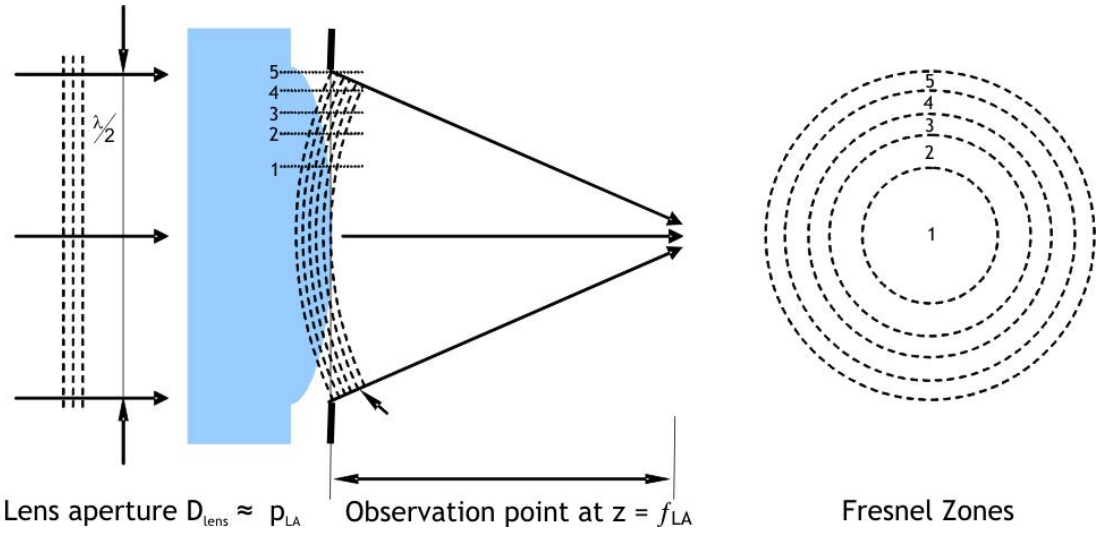

Fig. 3. Illustration of the Fresnel number.

With consideration of the flat-top dimension $D_{FT} = \frac{p_{LA} \cdot f_{FT}}{f_{LA}}$ and $D_{lens} \approx p_{LA}$ the Fresnel number *FN* of a microlens beam homogenizer [9] is defined as

$$FN \approx \frac{p_{LA} \cdot D_{FT}}{4 \cdot \lambda \cdot f_{FL}}, \tag{7}$$

whereas p_{LA} is the pitch of the microlens array, D_{FT} is the dimension of the flat-top intensity profile in the homogenization plane FP, f_{FL} is the focal length of the Fourier lens FL and λ is the wavelength.

Non-imaging homogenizers often show dominant diffraction effects due to Fresnel diffraction at the microlens array. The Fresnel diffraction is related to the Fresnel number *FN*. Higher Fresnel numbers give sharper edges and smaller variations of the flat-top profile. In practice, non-imaging homogenizers should have Fresnel numbers $FN > 10$, better $FN > 100$, to obtain a good uniformity. Non-imaging homogenizers are well suited for large area illumination, as the flat-top dimension D_{FT} is proportional to the Fresnel number *FN*. For small Fresnel numbers $FN < 10$ or high uniformity flat-top requirements, the imaging homogenizer is the preferred solution.

3.2 Spatial coherence in the case of a Fly's eye condenser

Fulfilling the image condition for imaging beam homogenizers holds a severe disadvantage for coherent laser beams. Microlens arrays are periodic structures, where the pitch p_{LA} is the grating period. Each microlens array will behave like

a diffraction grating and will generate diffraction orders with a period $\Lambda_{FP} = f_{FL} \cdot \lambda / p_{LA}$ in the homogenization plane FP. The influence of the partial spatial coherence onto the light distribution will be explained for the case of the Fly's eye condenser shown in Figure 4.

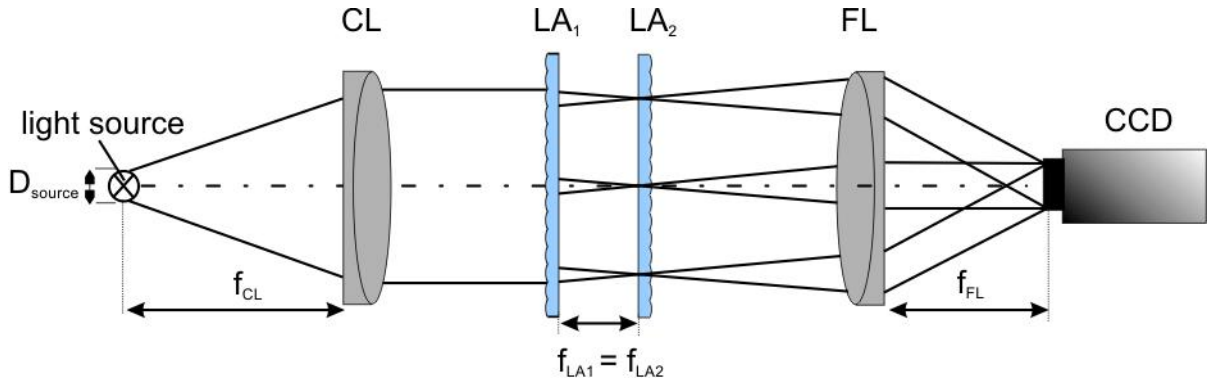

Fig. 4. Scheme of a Fly's eye condenser with identical microlens arrays.

Each point of the monochromatic, but spatially incoherent light source forms a plane wave with a certain tilt $\vartheta_{in} = x_{source} / f_{CL}$ (x_{source} is the distance of the light source point from the optical axis) behind the collimator lens CL. Each of these plane waves is incoherent to each other. In the wave-optical model each plane wave is split behind the first lens array LA_1 into several diffraction orders m_1. The period of the lens arrays LA_1 and LA_2 is p_{LA} and the wavelength of the light is λ. Then, the diffraction orders behind the first lens array propagate with the far field angle ϑ_1:

$$\vartheta_1 = \vartheta_{in} + m_1 \frac{\lambda}{p_{LA}}. \tag{8}$$

Here, only small angles are used ($p_{LA} >> \lambda$ for a typical microlens array) so that we can approximate $\sin\vartheta \approx \vartheta$. Behind the second microlens array LA_2 with the same period p_{LA} the diffraction orders m_2 have the same angular difference thus the far field angles ϑ_2 of the different diffraction orders behind the second microlens array are:

$$\vartheta_2 = \vartheta_1 + m_2 \frac{\lambda}{p_{LA}} = \vartheta_{in} + (m_1 + m_2) \frac{\lambda}{p_{LA}} = \vartheta_{in} + m \frac{\lambda}{p_{LA}}. \tag{9}$$

Finally, the Fourier lens FL focuses each plane wave of the different diffraction orders into a spot. This spot is in the focal plane at the lateral position:

$$x = \vartheta_2 f_{FL} = \vartheta_{in} f_{FL} + m \frac{\lambda}{p_{LA}} f_{FL}. \tag{10}$$

A wave-optical simulation of the intensity in the focal plane of Fourier lens FL for a single light source point is shown in Figure 5. For a circular diameter $Ø_{FL}$ of the illuminated aperture of Fourier lens FL each spot is of course an Airy disc (Figure 6) with a radius r_{Airy} between the central peak and the first minimum of:

$$r_{Airy} = 1.22 \frac{\lambda f_{FL}}{Ø_{FL}}. \tag{11}$$

Here, again the small angle approximation is used which is valid for $Ø_{FL} << f_{FL}$.

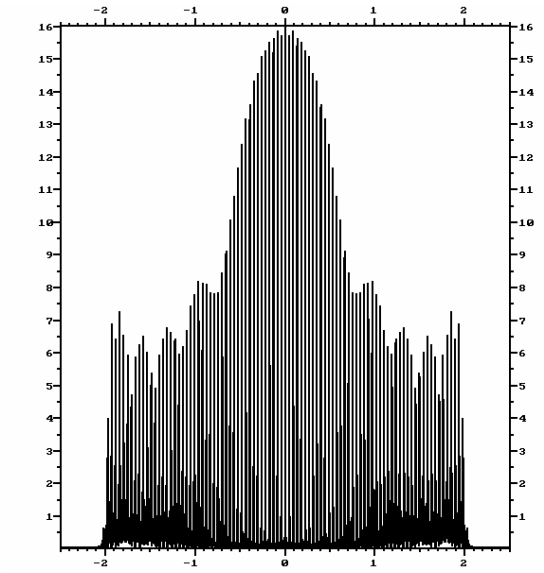

Fig. 5. Wave-optical simulation of the intensity in the focal plane of Fourier lens FL for a single light source point: total field in the focal plane.

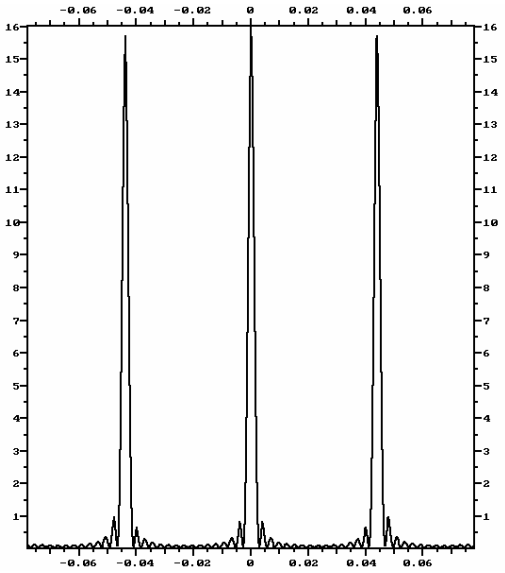

Fig. 6. Zoomed central part of Fig. 5 showing the single Airy discs of the different diffraction orders.

The intensities of the spot arrays in the focal plane of Fourier lens FL which are formed by different light source points are then added. Each light source point with axial distance x_{source} forms a laterally shifted spot array with a shift of $\Delta x = \vartheta_{in} f_{FL} = x_{source} f_{FL} / f_{CL}$. If the diameter D_{source} of the light source is such that the lateral shift Δx of all light source points is just one period Λ_{FP} of the spot array with $\Lambda_{FP} = \lambda f_{FL} / p_{LA}$, a smooth homogeneous intensity will be obtained in the focal plane of lens FL, if all light source points emit identically. However, if the diameter of the light source increases further there will be again high fluctuations of the intensity pattern. The simulated intensity distributions in the focal plane of lens FL for an extended light source for is shown in Figs. 7 and 8.

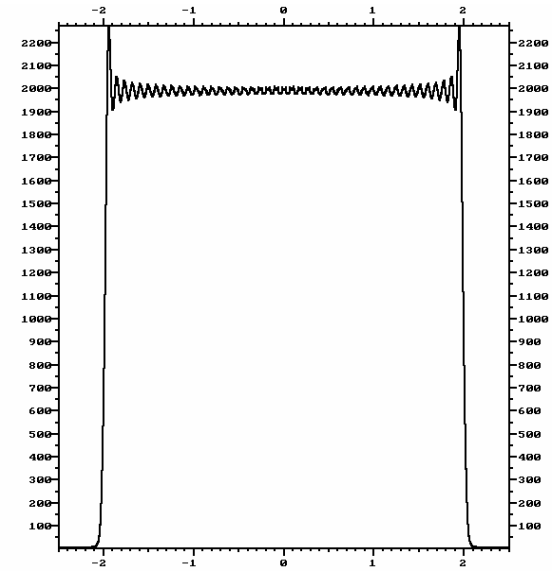

Fig. 7. Simulated intensity distributions in the focal plane for an extended light source $D_{source} / f_{CL} = \lambda / p_{LA}$.

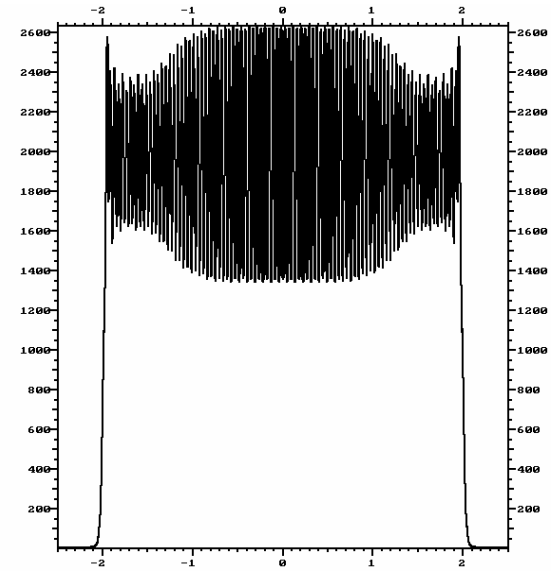

Fig. 8. Simulated intensity distributions in the focal plane for an extended light source $D_{source} / f_{CL} = 1.5\lambda / p_{LA}$.

Only in the case that the light source diameter is so large that the spot arrays of the different light source points are shifted by many periods there will be a nearly homogeneous intensity even if the light source diameter changes by a few percent or if the light source emits differently for different points. Figs. 9 and 10 show clearly this effect for a large light source with a ratio R of the angular extension of the light source $D_{\text{source}} / f_{\text{CL}}$ and of the angular extension of the spot array λ / p_{LA} of $R = 82$ or $R = 82.5$. There is nearly no difference between both intensity distributions. Only, by looking exactly on both Figures the right one shows a little bit higher fluctuations.

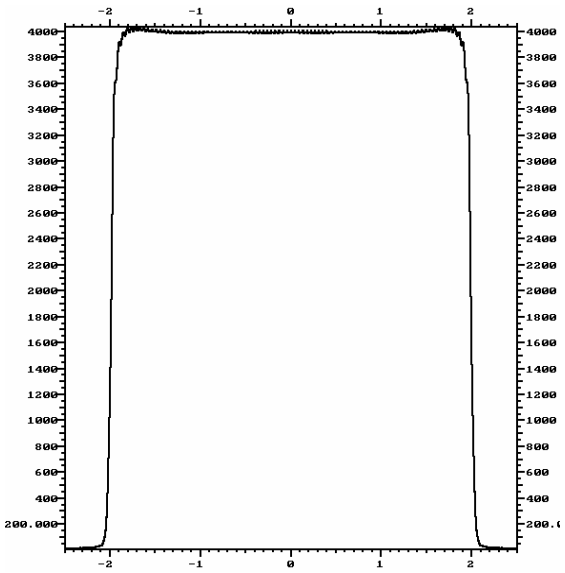

Fig. 9. Simulated intensity distributions in the focal plane of Fourier lens FL for a larger extended light extended light source $D_{source} / f_{CL} = 82\,\lambda / p_{LA}$.

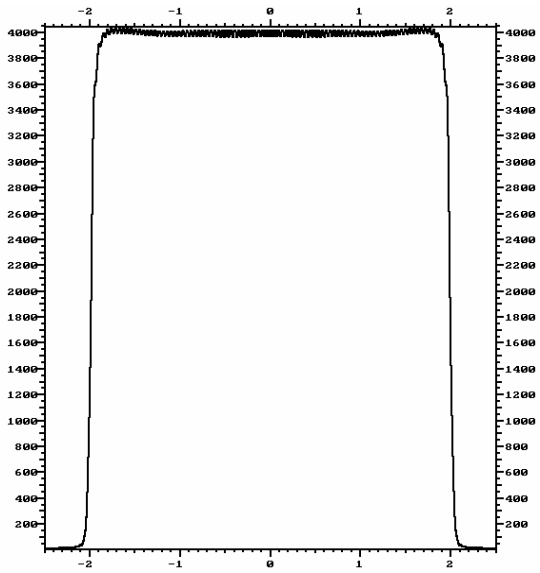

Fig. 10. Simulated intensity distributions in the focal plane of Fourier lens FL for a larger extended light extended light source $D_{source} / f_{CL} = 82.5\,\lambda / p_{LA}$.

Of course, there is an upper limit for the light source diameter depending on the lenses of the microlens arrays because the light source images which are formed by the collimator lens CL and the lens array LA_1 on the apertures of the lens array LA_2 are not allowed to be larger than one lens aperture of array LA_2. Otherwise, there will be cross talking between the different channels and the intensity distribution in the focal plane of Fourier lens FL will have undesired side bands. The maximum diameter of the light source which is allowed is:

$$D_{source}\,\frac{f_{LA1}}{f_{CL}} \le p_{LA} \;\Rightarrow\; R = \frac{D_{source} / f_{CL}}{\lambda / p_{LA}} \le \frac{{p_{LA}}^2}{\lambda f_{LA1}} = 4FN\,. \tag{12}$$

So, the ratio R which has to be large in order to have a good homogenization is limited by the Fresnel number FN of the lenses of the microlens arrays. Here, it is assumed that the lenses of the arrays have a diameter of one period. Consequently it is important that the Fresnel number of the microlenses is not too small, otherwise the homogenization cannot be uniform. Of course, the ratio R between the angular extension (field divergence of the light source) $D_{\text{source}}/f_{\text{CL}}$ of the light source and the diffraction angle λ/p_{LA} of the lens array is additionally limiting the homogenization, even if the Fresnel number of the lenses is larger. A spatially coherent or nearly spatially coherent light source cannot be homogenized sufficiently with a Fly's eye condenser using periodic lens arrays.

There is only one way to help in this case. By misadjusting the collimator lens CL in such a way that the extended light source is no longer exactly in its focal plane, a spherical wave will be formed by each point of the light source. Then, the interference pattern in the focal plane of Fourier lens FL for the different light source points will be of a higher frequency and more complex so that a slightly better homogenization can be achieved. The following Figures 11 and 12 show such a simulation which has to be compared with the upper Figures. Of course, this trick is only allowed to some extent because it smears out the flat top profile.

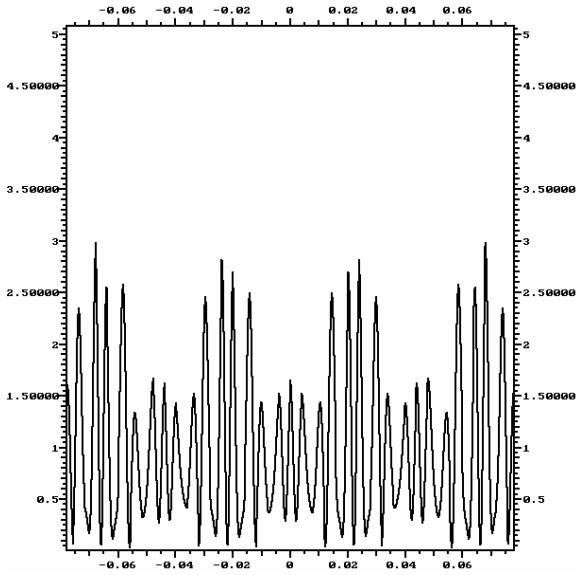

Fig. 11. Intensity distribution of one light source point if the collimator lens CL is axially misaligned so that spherical waves enter the lens arrays.

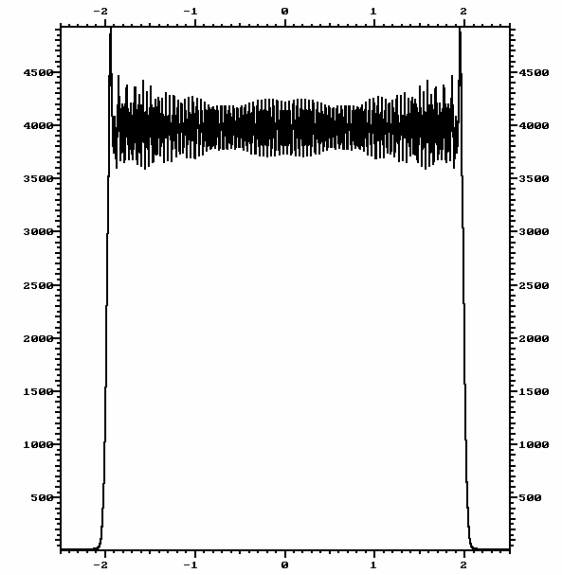

Fig. 12. Intensity distribution for an extended light source for the case $D_{source} / f_{CL} = 1.5\lambda / p_{LA}$ if the collimator lens CL is axially misaligned so that spherical waves enter the lens arrays.

The spot patterns generated by grating diffraction and interference could be reduced by different measures. A larger microlens pitch p_{LA} leads to a finer period Λ_{FP} in the Fourier plane. A detuning of beam homogenizer components, e. g. a shift of the microlens arrays or the working plane out of its correct positions allows a reduction of the modulation of the flat top profile.

These grating interference effects can be demonstrated with a fly's eye condenser and an illumination with a collimated diode-laser beam at a wavelength of 670 nm. The results are shown in Fig. 13. The pitch p_{LA} of the used microlens array is 0.3 mm. The results show a good agreement with theoretical calculations. The period of the spots is approximately 677 µm for a Fourier lens focal length of 300 mm.

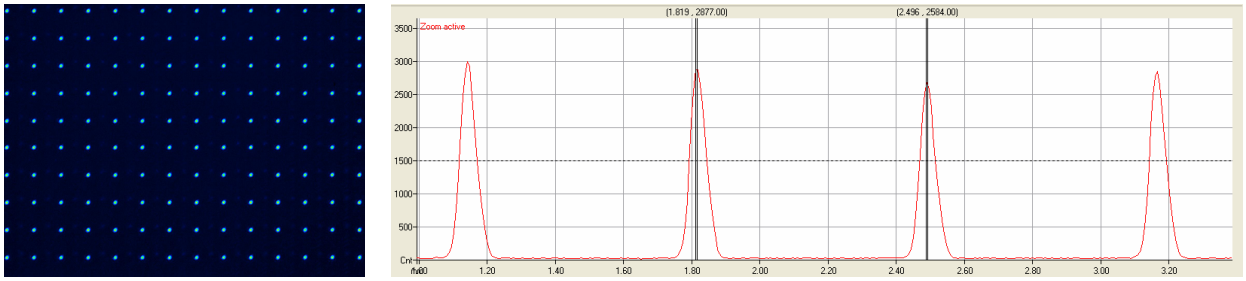

Fig. 13. Measured intensity profile at focal plane of the Fourier lens.

3.3 Diffusers

As discussed above, effects like grating interference and speckles are well correlated with the coherence of a laser beam. A laser with many incoherent modes (larger M^2) will have lower contrast speckle than a single-mode coherent laser. A reduction of coherence related effects by using rotating or static diffuser plates is possible for applications where light for a cw laser, or multiple pulses from a pulsed laser, are integrated at the detector or object. The diffusers can be fabricated in fused silica for wavelengths between ultraviolet and near infrared or silicon for the middle infrared. The scattering angle can be influenced by processing parameters and is typical between 1° and 20°. Figure 14 shows the angular light distribution of a structured fused silica diffuser in comparison to a typical ground glass diffuser.

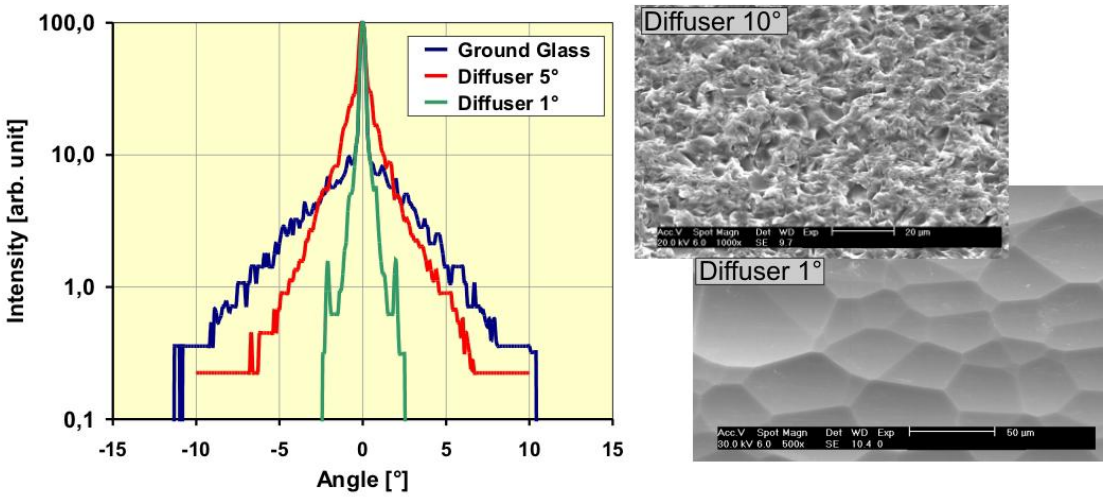

Fig. 14. Angular distribution of ground glass and structured fused silica, SEM pictures of diffuser surface.

The rotating diffuser plate is usually placed in a separate telescope near the common focus plane (Fig. 15). The diffuser plate is rotating, thus the speckle pattern is changing temporally. By shifting the diffuser position or detuning the telescope, the source divergence is changed. Time-averaged, the light emitting from the rotating diffuser is similar to an incoherent extended light source. Placing the diffuser near the focus of the beam, e. g. by using a beam expander in front of the homogenizer, reduces the coherence by creating a new extended light source, whereas the size of the source is equal to the spot diameter on the rotating diffuser. Unfortunately rotating diffusers do not work for pulsed lasers like Nd:YAG with nano- or picosecond pulses. For single pulse exposure different measures, such as stair case beam splitters and pulse stretchers are applied.

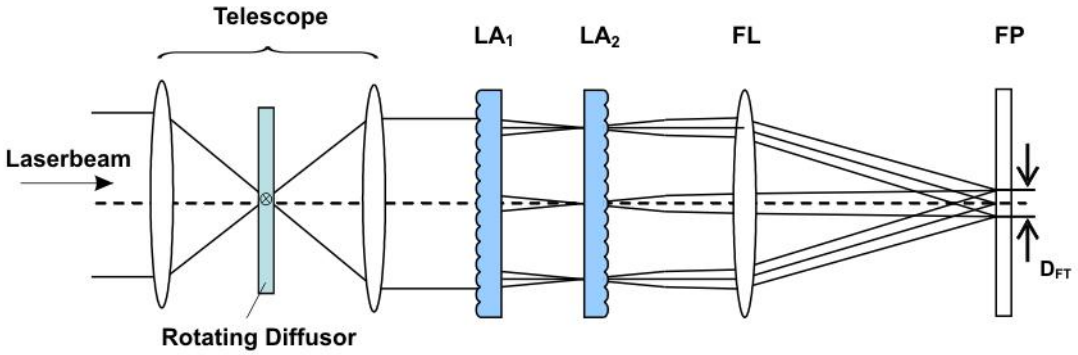

Fig. 15. Schematic setup of a rotating diffuser used with a microlens homogenizer.

Experimental results of the application of a diffuser within a microlens homogenizer in a fly's eye setup are shown in Figures 16 and 17. A diode laser with a wavelength of 670 nm is used. The pitch of the micro lens array is 250 µm. A Fourier lens with a focal length of 40 mm generates a flat-top with dimensions of approx. 6.4 x 6.4 mm^2. For this configuration the Fresnel number is approx. 15. It can be demonstrated that the grating effects can be smoothed with the application of a rotating diffuser. With a good alignment the beam uniformity is in the range of ± 5 % and is better than ± 1% with an incoherent illumination.

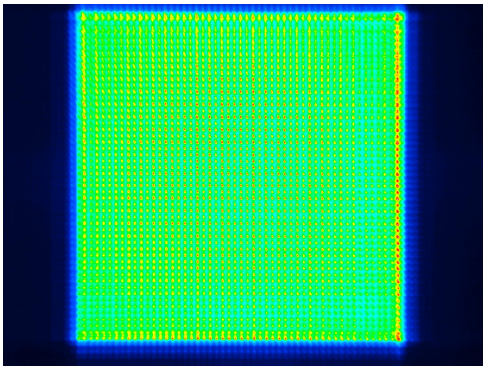

Fig. 16. Intensity distribution distributions in the focal plane of Fourier lens FL without the application of a rotating diffuser.

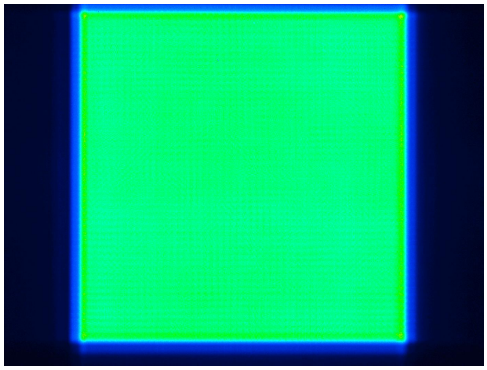

Fig. 17. Intensity distribution distributions in the focal plane of Fourier lens FL: smoothing of interference spikes by application of a rotating diffuser.

The 2-D diffusers shown in Figure 14 are of very limited use for thin-line homogenizers. 1D random diffusers consisting of a random pattern of arbitrary and statistically placed diffusing elements are under investigation. These diffusers are used to improve the uniformity of line homogenizers and laser light sheets.

4. MICROLENS BEAM HOMOGENIZER APPLICATIONS

4.1 Light Sheet Homogenizer

Planar laser diagnostics means a spatial high-resolution measurement of the 2 dimensional concentration distribution of gases or fluids, which are excited by pulsed lasers, for example Excimer lasers [3]. Therefore a thin laser light sheet is established within the media which has to be investigated. The fluorescence signal of the tracing substance, which is excited by laser irradiation, is detected with a high resolution ccd-camera. A schematic setup is shown in Figure 18.

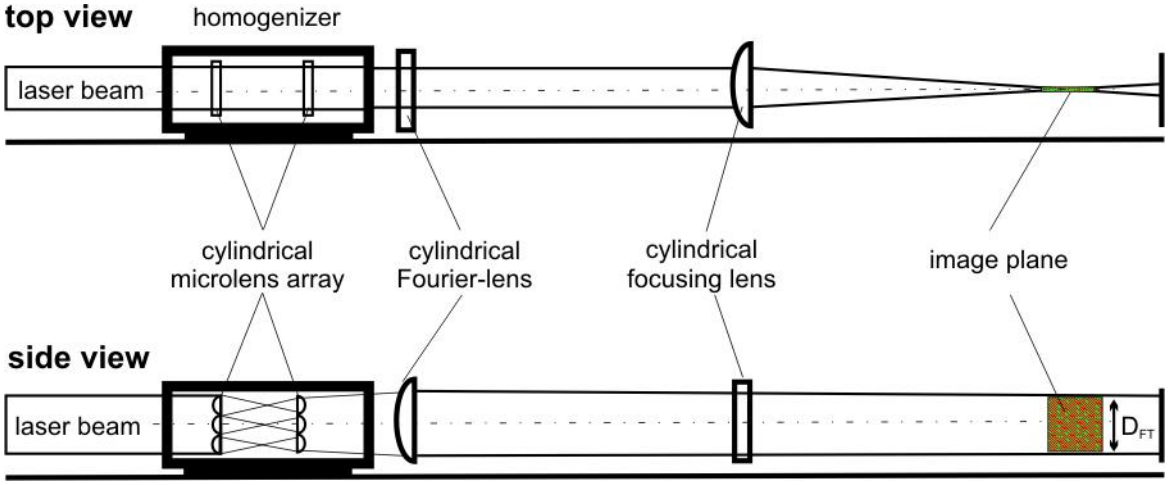

Fig. 18. Setup of the light sheet homogenizer.

The detected signal is directly proportional to the absolute concentration of the tracer substance and therefore to the concentration of the carrying fluid. To investigate the absolute concentration out of single pictures, a homogeneous intensity distribution in the image plane is necessary. Indeed spatial inhomogeneity can be corrected after measurement but this procedure is very time consuming. Temporal fluctuations and hot-spots cannot be corrected. The homogenizer consists of two cylindrical microlens arrays with a pitch of 0.5 mm. The plano-convex Fourier lens generates a flat-top with a size of approximately 50 mm. The second beam direction is focussed by a lens.

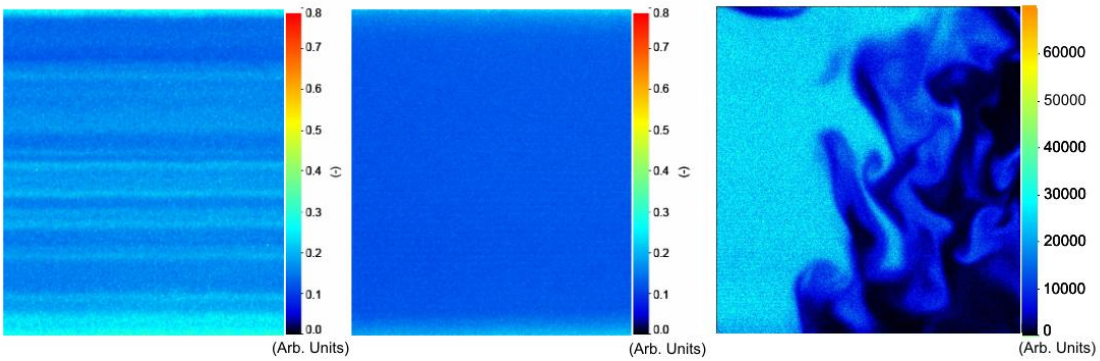

Fig. 19. RMS image of the normalized fluorescence signal: left: without the application of the beam-homogenizer. middle: with the application of the beam-homogenizer. Right: tracer-LIF measurement of the mixing field of two different turbulent flows (by courtesy of the research group of Lehrstuhl für Technische Thermodynamik Friedrich-Alexander Universität Erlangen-Nürnberg, Germany).

Figure 19 shows examples of camera pictures of a planar laser induced fluorescence with and without a homogenizer. The intensity distribution without homogenizer shows stripes, which can be traced back to the instable resonator type of the Excimer laser (Excimer laser wavelength 248 nm, pulse energy 250 mJ). The tracer-LIF measurement of the mixing field of two different turbulent flows is shown in the right camera picture of Figure 19.

4.2 Laser Micro Machining

A homogenizer for illumination of a mask is used within an ArF-Excimer laser working station. Due to the short operation wavelength of 193 nm, the maximum pulse energy of 120 mJ and the peak power of 7 MW, the homogenizer material is a high purity grade fused silica with low absorption and degradation at this wavelength. Furthermore the telescope homogenizer setup with two different microlens arrays has to be used to reduce the energy density at the second microlens array. The typical raw beam profile of the Excimer laser with a Gaussian intensity distribution in the x-direction and super-Gaussian in y-direction is shown in Figure 20. The dimension of the laser beam is approx. 5 x 14 mm with a beam divergence of 1 x 2 mrad. For conversion of the ultraviolet radiation into visible and detectable light a special fluorescence plate is used.

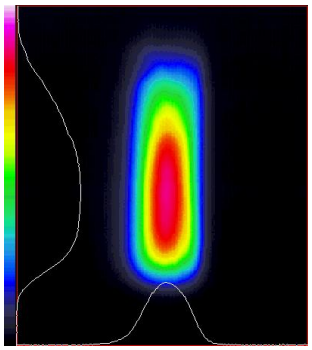

Fig. 20. Measured intensity distribution of Excimer laser raw beam.

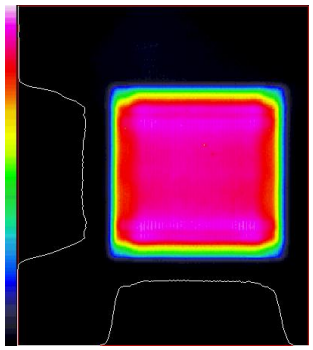

Fig. 21. Measured intensity distribution of homogenized beam.

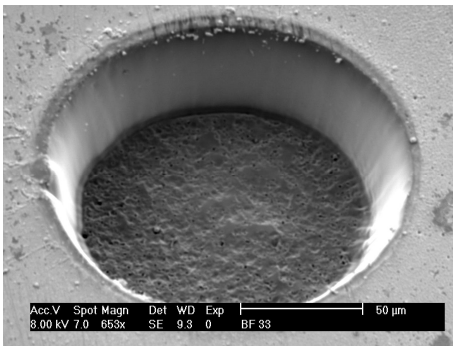

Fig. 22. SEM picture of laser ablation in borosilicate glass.

We used two square microlens arrays with a pitch of 0.3 mm and a focal length of 3.9 mm and 7 mm. The focal length of the spherical Fourier lens is 175 mm. A square flat-top with dimensions of approx. 7.5 x 7.5 mm² and beam uniformity (measured with the norm ISO 13694) of better than ± 5% is realized (Fig. 21). The illuminated mask with a drilling diameter of 600 µm is projected with a demagnification factor of approx. 4 onto the glass substrate (borosilicate). The ablation which is shown in Figure 22 shows a very smooth ablation ground and sharp edges.

5. CONCLUSION

We showed capabilities and limits of microlens arrays for shaping laser beams into homogeneous patterns like light sheets or flat-tops. Design rules which consider geometrical and physical optics were presented. We demonstrated a simple estimation of diffraction influence with calculating the Fresnel number of the system. Furthermore we presented a useful method for reducing interference patterns with the application of a rotating random diffuser. Examples of the usage of microlens beam homogenizer in planar laser diagnostic and Excimer laser micromachining were shown.

REFERENCES

1. R. Völkel, H. P. Herzig, P. Nussbaum and R. Dändliker, "Microlensarray imaging system for photolithography," Optical Engineering 45 (11), 3323 – 3330 (1996).
2. U. Popp, Th. Neudecker, U. Engel, M. Geiger, "Excimer Laser Texturing of Hard Coated Cold Forging Tools - Investigations on Tool Life," Advanced Technology of Plasticity 2002, Vol. II., 1633-1638 (2002).
3. S. Pfadler, F. Beyrau, M. Löffler, and A. Leipertz, "Application of a beam homogenizer to planar laser diagnostics," Optics Express 14, 10171-10180 (2006).
4. J. A. Hoffnagle and C. M. Jefferson, "Design and Performance of a Refractive Optical System that Converts a Gaussian to a Flattop Beam," Appl. Opt. 39, 5488-5499 (2000).
5. T. Kajava, M. Kaivola, J. Turunen, P. Paakkoned, M. Kuittinen, P. Laakkonen and J. Simonen, "Excimer laser beam shaping using diffractive optics," Lasers and Electro-Optics Europe, 2000. Conference Digest. 2000 Conference on Volume, Issue, 2000 Page(s): 1 pp. (2000).
6. I. Harder, M. Lano, N. Lindlein and J. Schwider, "Homogenization and beam shaping with micro lens arrays," Photon n Management, Proceedings of SPIE, 5456, 99-107 (2004).
7. K. Räntsch, L. Bertele, H. Sauer and A. Merz, "Illuminating System," US-Patent 2186123, United States Patent Office, 1940.
8. A. Büttner and U. Zeitner, "Wave optical analysis of light-emitting diode beam shaping using microlens arrays," Optical Engineering 41 (10), 2393 – 2401 (2002).
9. Fred M. Dickey and Scott C. Holswade, *Laser Beam Shaping: Theory and Techniques*, Publisher: Marcel Dekker, (2000).
10. B. Besold and N. Lindlein, "Fractional Talbot effect for periodic microlens arrays," Optical Engineering 36 (4), 1099-1105 (1997).
11. F. Wippermann, U.D. Zeitner, P. Dannberg, A. Bräuer and S. Sinzinger, "Beam homogenizers based on chirped microlens arrays," Optics Express 15, 6218-6231 (2007).